ACS NANO

www.acsnano.org

PERSPECTIVE

Single-Molecule Surface-Enhanced Raman Spectroscopy: Challenges, Opportunities, and Future Directions

Makayla Maxine Schmidt, Alexandre G. Brolo,* and Nathan C. Lindquist*

Cite This: *ACS Nano* 2024, 18, 25930–25938

Read Online

ACCESS | Metrics & More | Article Recommendations

ABSTRACT: **Single-molecule surface-enhanced Raman spectroscopy (SM-SERS) is a powerful experimental technique for label-free sensing, imaging, and chemical analysis. Although Raman spectroscopy itself is an extremely "feeble" phenomenon, the intense interaction of optical fields with metallic nanostructures in the form of plasmonic hotspots can generate Raman signals from single molecules. While what constitutes a true single-molecule signal has taken some years for the scientific community to establish, many SERS experiments, even those not specifically attempting single-molecule sensitivity, have observed fluctuation in both the SERS intensity and spectral features. In this Perspective, we discuss the impact that fluctuating SERS signals have had on the continuing advancement of SM-SERS, along with challenges and current and potential future applications.**

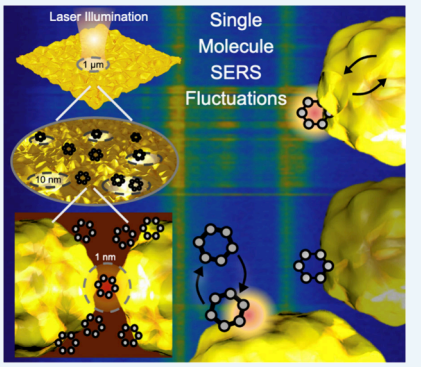

KEYWORDS: *Single-Molecule Surface, Enhanced Raman Spectroscopy, SERS Fluctuations, High-Speed Spectroscopy, Super-Resolution Imaging*

Ever since the report in 1974 on the increase in Raman signal from pyridine adsorbed onto a roughened silver electrode[1] and the discovery in 1977 of a million-fold enhancement in signal from what would be expected given the number of illuminated molecules, surface-enhanced Raman spectroscopy (SERS) has become one of the most active research areas in the fields of chemistry, physics, optics, materials science, and nanotechnology. During the late 1990s, SERS was calculated to provide even higher enhancements, potentially a million-million-fold, provoking scientists to determine whether it could truly be a single-molecule-sensitive technique. To explain the SERS effect and its exquisite sensitivity, the concept of the plasmonic "hotspot" has become central to its interpretation,[2] giving an electromagnetic enhancement effect.[3] These hotspots are created by illuminating metallic nanostructures with light, as illustrated in Figure 1a. Nanostructure geometry ranges from randomly roughened silver surfaces to carefully fabricated arrays of nanoantennas[4] and to solution-grown nanospheres, nanoshells, nanostars, and nanocrystals.[5] In all cases, the plasmon resonances of these structures effectively squeeze electromagnetic energy into very small volumes, with an accompanying increase in optical intensity, thereby rendering the surface "SERS active". Decades of research have been done to improve the reliability and effectiveness of these substrates,[4] with some substrates having been commercialized.[6] Depending on the substrate, these plasmonic hotspots can range in size from tens of nanometers, as seen in Figure 1b, down to the atomic "picocavity" scale,[7] as seen in Figure 1c, and are able to generate SERS signals from single molecules[8,9] or even single vibrational modes within a single molecule.[10]

Interestingly, while SERS quickly established itself as a powerful analysis technique, many observations noted that the signals sometimes displayed significant fluctuations in both signal intensity and spectral features.[11] Early interpretations of these SERS Intensity Fluctuations (SIFs) were assigned to a single-molecule phenomenon,[12−15] although a full interpretation of what constituted genuine single-molecule (SM) SERS remained controversial.[16] In time, SM-SERS has become firmly established via multiple experimental techniques, including several definitive experiments done with two analytes[17] or isotopologues,[18] and the origin of these single-molecule

Received: July 15, 2024
Revised: August 26, 2024
Accepted: August 29, 2024
Published: September 11, 2024

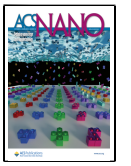

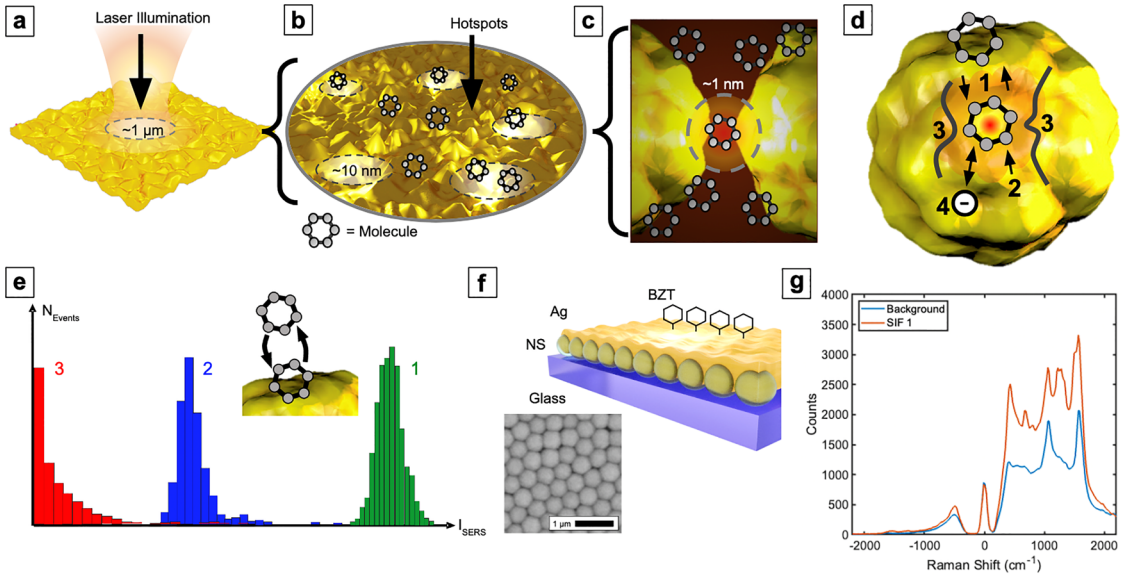

Figure 1. Essential concepts for single-molecule SERS. (a) A typical SERS experiment will use a rough metallic film or an arrangement of nanoparticles. The focused laser spot size will be around ~1 μm. (b) Single molecules on the surface encounter plasmonic hotspots on the ~10 nm scale. If the concentration of molecules is small enough and there are enough hotspots, single-molecule SERS events can be observed. (c) Single molecules on the ~1 nm scale can be excited by the smallest and most intense hotspots, even if the rest of the surface is saturated with molecules. (d) Various mechanisms for the observed intensity fluctuations in SM-SERS: (1) adsorption/desorption of a single molecule into a hotspot; (2) surface diffusion of the molecule; (3) dynamic creation of a hotspot due to motion of metallic adatoms; (4) various chemical contributions such as charge transfer processes. (e) Typical SERS intensity distribution plots according to concentration. Each histogram (shifted across the *x*-axis to prevent superimposing) corresponds to rhodamine 6G adsorbed on a SERS silver surface at the concentrations of (1) 5 μM, (2) 100 nM, and (3) 10 nM. (1) At high concentration, the intensity distribution has normal behavior. (2) As the concentration decreases, the hotspots that are the most efficient begin to have a stronger influence on the SERS signal, resulting in an asymmetric tail in the intensity distribution toward higher intensities. (3) Approaching the single-molecule regime of concentration results in a power-law probability distribution with a small number of intense, single-molecule events. (f) Illustration of a SERS substrate, with benzenethiol (BZT) as the probe molecule coating an Ag film-over nanosphere (FoN) sample. (f inset) SEM image of the sample surface topography, showing gaps between spheres that promote good SERS activity. (g) Sample SIF spectrum compared to background, or average, SERS spectrum of BZT. Figure panels adapted with permission from refs 20, 21, 25, and 26. Copyright 2019 Nature and 2009, 2021, and 2023 American Chemical Society.

fluctuations has been assigned to a variety of dynamic and complex processes, including molecular adsorption/desorption, surface diffusion, molecular reorientation,[19] thermal effects,[15] and metal surface reconstruction, as illustrated in Figure 1d.[20] Each of these processes can contribute to a fluctuating signal depending on the various experimental parameters. For example, for an experiment done in solution, adsorption/desorption of the probe molecule would likely be the dominant cause of the fluctuations.[21,22] However, in a sample that is completely dry and saturated with probe molecules, as is done with self-assembled monolayers and shown in Figure 1f,g, the cause of fluctuations is a bit more obscured, since surface mobility is assumed to be minimal. In this case, the concept of an intense, localized, yet *static* hotspot has come into question. Recent experiments have also shown these SERS intensity fluctuations to occur over an extremely wide range of time scales, from seconds to microseconds.[20,23] In the picocavity regime, it is the direct interactions between mobile metallic adatoms and the probe molecule, driven by the incident light, that cause dynamic signals.[10] Therefore, the underlying source of all SERS fluctuations is likely to be a complex interplay of several different effects that occur at different time scales and under different experimental conditions. While it remains true that a fluctuating SERS signal is not definitive proof of single-molecule behavior, in that several molecules could still be contributing to a fluctuating signal at any given time, it is true that single-molecule experiments will naturally fluctuate, as seen in the rich history of single-molecule fluorescence.[24] Indeed, since SERS fluctuations are readily observed across a wide range of experimental conditions, dynamic behavior appears to be a fundamental characteristic of the SERS effect. In this Perspective, we outline experimental observations of SM-SERS, the current understanding of signal fluctuations as a single-molecule phenomenon, and the expanding notion of the nature of the plasmonic hotspot itself. We also discuss the many current and potential future applications, ranging from medical diagnostics to environmental monitoring and to biosensing and imaging.

EXPERIMENTAL CONDITIONS FOR SM-SERS

SM-SERS has been observed with a variety of experimental designs,[27] such as samples with a low concentration of probe molecules in solution,[22] dry samples with self-assembled monolayers,[28] and high-speed acquisition systems,[20] and is even thought to be quite common in many SERS experiments.[17] In addition, SIFs from dried samples with a low concentration of probe molecules have been used for high-resolution imaging purposes.[29] As discussed above, SM-SERS signals often show significant fluctuations, in both intensity and spectral features. The most straightforward interpretation of these fluctuations is that a single molecule in solution will diffuse in and out of a single hotspot. It has been shown that the concentration of molecules in solution will affect the SM-

https://doi.org/10.1021/acsnano.4c09483
ACS Nano 2024, 18, 25930−25938

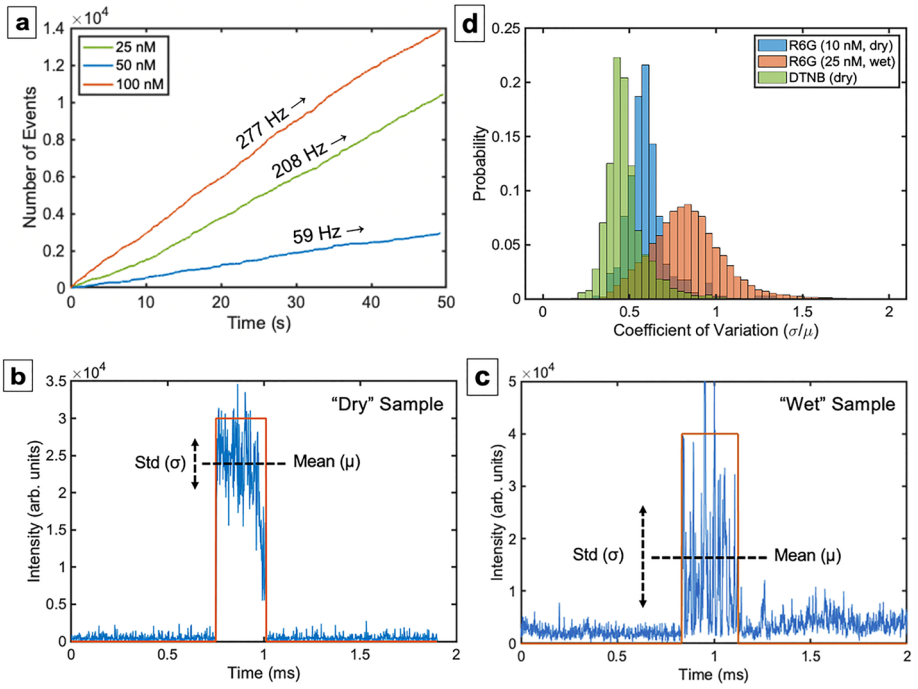

Figure 2. High-speed SERS fluctuations from "wet" and "dry" nanoparticle clusters. (a) Investigating the effect of probe molecule concentration on the average rate of SERS fluctuations, i.e., the SIF event rate, for three different concentrations of R6G in solution. The 100 nM solution has a higher average SIF rate than the 50 nM solution, but it is not exactly doubled. In addition, the average SIF rate for the 25 nM solution is almost as high as the rate for the 100 nM solution. This is likely due to varying numbers of hotspots that were illuminated in each sample, rather than a varying concentration of molecules. (b) A sample SIF from the "dry" sample incubated first in 10 nM R6G and then dried. This SIF displays a distinct ON/OFF characteristic compared to (c) a sample SIF from a "wet" sample of 25 nM R6G which was more noisy. (d) Histogram displaying the coefficient of variation (standard deviation divided by the mean) for three different sample types on Ag nanoclusters: "wet" R6G, "dry" R6G, and a "dry" 5,5′-dithiobis(2-nitrobenzoic acid) (DTNB) monolayer. The "wet" sample displayed the most variation and a wider distribution than the two "dry" samples. Figure adapted with permission from ref 22. Copyright 2022 American Chemical Society.

SERS signal, solidifying this conclusion. In fact, lowering the concentration of the probe molecule will transition the SERS signal to single-molecule statistics. This is shown in Figure 1e, where rhodamine 6G (R6G) adsorbs and desorbs on a SERS-active silver surface at concentrations of 5 μM, 100 nM, and 10 nM, and the resulting SERS intensity distributions are compared. At high concentrations, the intensity distribution of the SERS signal has normal behavior. As the concentration decreases, the plasmonic hotspots that are the most efficient begin to have a stronger influence on the SERS signal, resulting in an asymmetric tail toward higher intensities in the intensity distribution. The lowest concentration, approaching the single-molecule regime, results in a power-law probability distribution with a small number of intense single-molecule events. Probe molecule concentration is not, however, the only variable affecting the SIF fluctuation rate. The graph in Figure 2a displays data comparing probe molecule concentration and the average *rate* (instead of *intensity*) of the SERS fluctuations for Ag nanoclusters and three different R6G concentrations in solutions of 100, 50, and 25 nM. The 100 nM solution has a higher, but not double, average rate of SERS fluctuations than the 50 nM solution. Adding further complexity, the average rate of SERS fluctuations for the 25 nM solution is nearly as high as the rate for the 100 nM solution. This unexpected outcome is likely due to varying numbers of plasmonic hotspots that were illuminated in each of the three samples, further emphasizing the complex, multivariable interplay of factors behind SIF behavior.

Many early SM-SERS experiments focused on samples with low concentrations of probe molecules (<100 nM) in order to have only one molecule present at the hotspot location at a time,[30] but further investigations revealed that SM-SERS can be observed with a much wider variety of experimental designs, such as dry samples with highly concentrated probe molecules.[28] While the wet sample is expected to have SIFs due to the freely floating probe molecule moving in and out of the plasmonic hotspot, the dry sample is also expected to have SIFs due to transient hotspot generation caused by the mobility of metallic atoms. Figure 2b–d shows an example of comparing the SIF behavior between the experimental conditions of dry and wet samples.[22] A sample SIF from the dry sample, seen in Figure 2b, displays clear ON and OFF characteristics with little noise, whereas a sample SIF from the wet sample, shown in Figure 2d, displays far more noise within a single SIF event. The coefficients of variation histograms displayed in Figure 2d show that the wet samples displayed on average more variation and a wider distribution of intensities, indicating that the SERS signal from the wet samples fluctuated more during a single SIF event than the signal from the dry samples. In other words, the SIFs from the wet samples were "noisier". In regard to the length of SIF duration, the SIF events from the dry samples were on average slightly longer than the SIF events from the wet samples. This was expected due to the more "fixed" nature of the probe molecules on the dry samples. The average rate of SERS fluctuations in the wet samples seemed to depend more on the number of

https://doi.org/10.1021/acsnano.4c09483
ACS Nano 2024, 18, 25930−25938

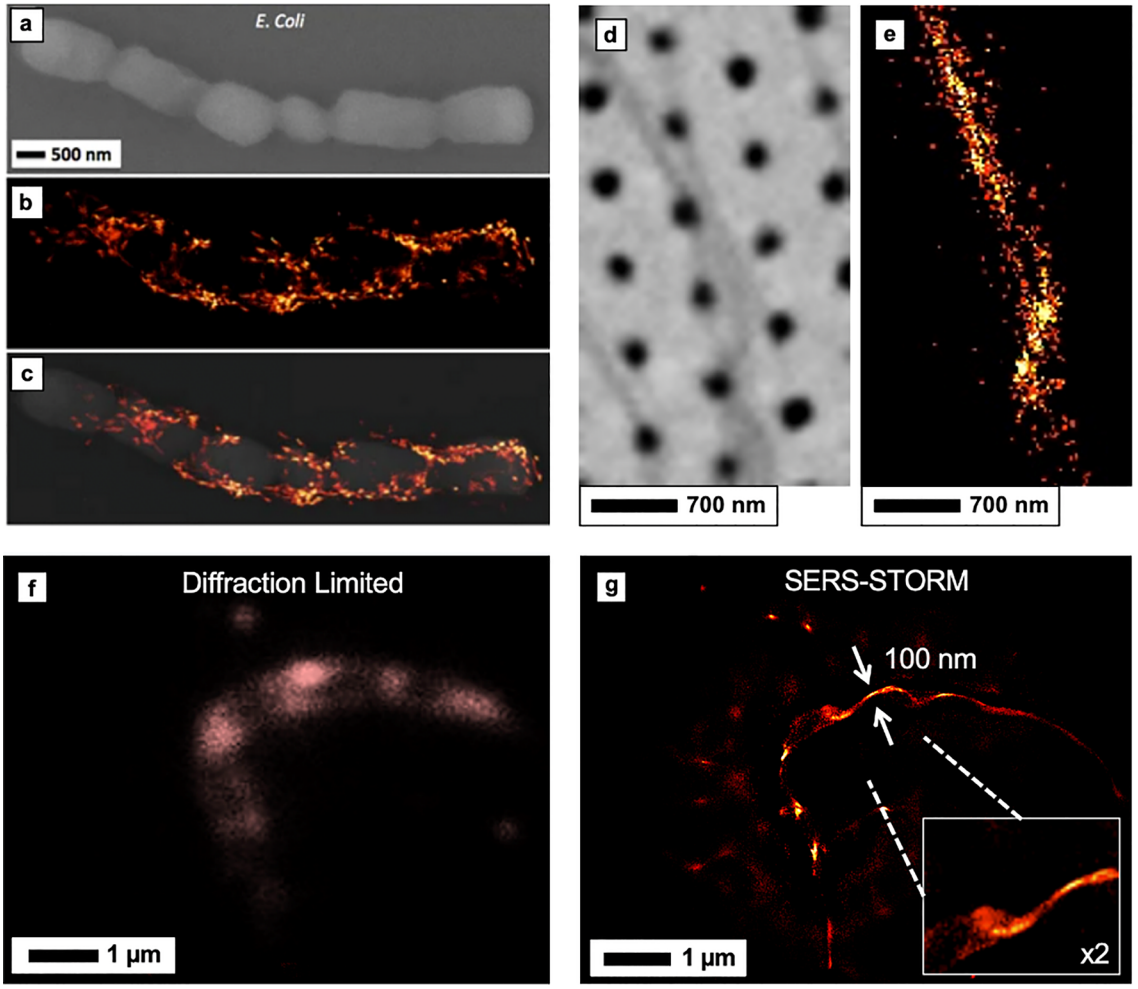

Figure 3. Super-resolution SERS imaging using SIFs. (a) *E. coli* on an ultrathin rough Ag surface imaged using SEM and (b) SERS-STORM. (c) The two imaging techniques overlaid. (d) Collagen fiber on plasmonic nanohole array imaged using SEM and (e) SERS-STORM. The two imaging methods again are in good agreement. (f) Diffraction-limited SERS image of a collagen fiber on a nanohole array. (g) SERS-STORM algorithm used to achieve super-resolution imaging of the same collagen fiber. Figure adapted with permission from refs 29 and 35. Copyright 2017 Nature and 2016 American Chemical Society.

active hotspots on the sample than on the concentration of the probe molecule.[22] Overall, the statistical analysis of SIFs can be seen to provide insight into the interactions between probe molecules and plasmonic hotspot activity.[31]

OPPORTUNITIES FOR SENSING AND IMAGING

Since the plasmonic hotspots are deeply subwavelength, one exciting application is using them for super-resolution imaging.[32] This can take many forms, including directly scanning a single hotspot over a substrate,[33] as is done with tip-enhanced Raman spectroscopy (TERS), or using a substrate with a distribution of hotspots to effectively illuminate subwavelength features of a sample. One form of imaging exploits the fluctuations of the SERS signal, borrowing concepts from stochastic optical reconstruction microscopy (STORM), a super-resolution technique developed for fluorescence imaging.[34] As the SERS signal fluctuates in time, each event is localized with a precision approaching a few nanometers.[29,35] In this way, SERS-STORM can build up an image of the substrate/sample interaction, visualizing sub-wavelength structures while at the same time collecting chemical information. It is therefore possible to have, for example, a single nanoslit illuminate a single nucleobase for SERS-based nanopore sequencing and imaging.[36] SERS-based hyperspectral imaging has shown potential for the detection of cancer biomarkers[37] and has been used to monitor plasmon-assisted chemical reactions with single-molecule sensitivity.[38] These "label-free" forms of super-resolution chemical imaging have also been used to visualize cell membranes and other biological structures.[39] Figure 3 shows SERS-STORM imaging used to visualize both collagen fibers and various bacterial species.[29,35] Figure 3a–c display *E. coli* bacteria on an ultrathin Ag film. SEM and SERS-STORM imaging techniques showed good agreement. Collagen fibers on a plasmonic nanohole array were also imaged using SEM and SERS-STORM techniques, as seen in Figure 3d,e, respectively. Figure 3f displays a diffraction-limited SERS image taken of the same collagen fiber sample, and Figure 3g shows how the SERS-STORM algorithm can create a super-resolution imaging of the same sample.[35] Furthermore, the spectral capability of SERS allows, for example, label-free diagnostics of bacterial species that may have otherwise required staining to be identified.[29] The ability of SERS-STORM and related imaging techniques[32] to collect both spectral data and conduct high-resolution imaging makes this technology a promising tool for bioimaging and biosensing.

https://doi.org/10.1021/acsnano.4c09483
ACS Nano 2024, 18, 25930–25938

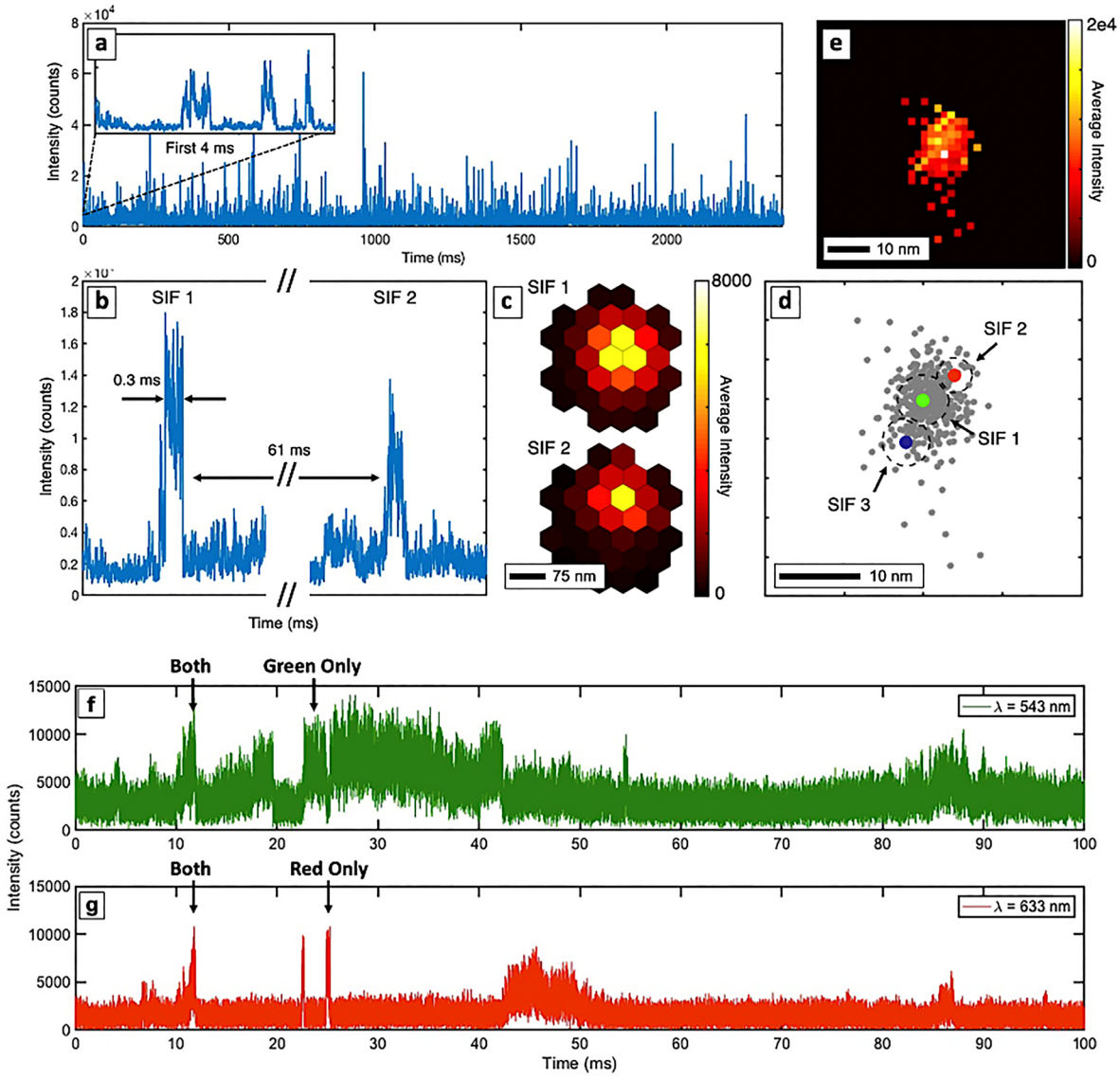

Figure 4. High-speed SERS intensity fluctuations with temporal, spatial, and wavelength dependence. (a) SIFs recorded at high speeds over 2.5 s, with many SIFs occurring on the submillisecond time scale. The spectral range of this specific intensity acquisition is integrated over 500 cm^{-1} to ~2000 cm^{-1}. (b) Two SIFs, occurring 61 ms apart and each lasting approximately 0.3 ms. (c) High-resolution imaging using a PMT array detector allows for imaging of the SIF point spread function. Two SIF events can be seen occurring at different locations on the nanoparticle. (d) SIF events accumulated spatially over time to create an overall image of the nanoparticle, as displayed by the gray dots. Three individual SIF events are highlighted, occurring within ~7 nm of each other. The dotted rings around the three events depict the standard deviation of the fit location, derived from the multiple frames of each event. (e) Average localized SERS intensity signal across the surface of a nanoparticle. (f,g) Wavelength dependence of SERS signal intensity from a SiO_2/Ag nanoshell obtained using a dual-channel time-series scan with (f) a 543 nm excitation laser and (g) a 633 nm excitation laser. The two channels of the scan run simultaneously, allowing for determining which SIFs correspond to each (or both) excitation wavelength. Both channels have a spectral range from 1250 to 1450 cm^{-1}. Figure adapted with permission from ref 20. Copyright 2019 Nature.

SPATIAL AND SPECTRAL CHARACTERIZATION OF HIGH-SPEED SERS FLUCTUATIONS

The fast acquisition time of the SERS signal has provided information about the behavior of single-molecule SIFs. Figure 4 shows an example of using a high-speed super-resolution imaging technique to gain insight into both the spatial and temporal characteristics of single-molecule SERS intensity fluctuations from dry, fully coated Ag nanoshell samples.[20] The data shown in Figure 4 were acquired at a rate of 800000 frames per second and had a spatial resolution of approximately 7 nm. In these experiments, spectral information was lost due to the use of high-speed photomultiplier tube (PMT) detectors. However, by utilizing this fast acquisition rate, shown in Figure 4a, SIFs as brief as 10 ms were identified. This temporal resolution also revealed that many of the nanoparticles were SERS-inactive for over 90% of the time, as seen in Figure 4b, suggesting that the fluctuations themselves are causing the dominant overall SERS signal.[20] This high-speed phenomenon could not be observed on an apparatus with the typical slower acquisition rate (~1 Hz), as the fluctuations would average out. The capabilities of the high-speed imaging system, using an array of PMT detectors, are shown in Figure 4c. This allowed capturing data on the specific locations of the SIF events as seen in Figure 4d, which displays

https://doi.org/10.1021/acsnano.4c09483
ACS Nano 2024, 18, 25930−25938

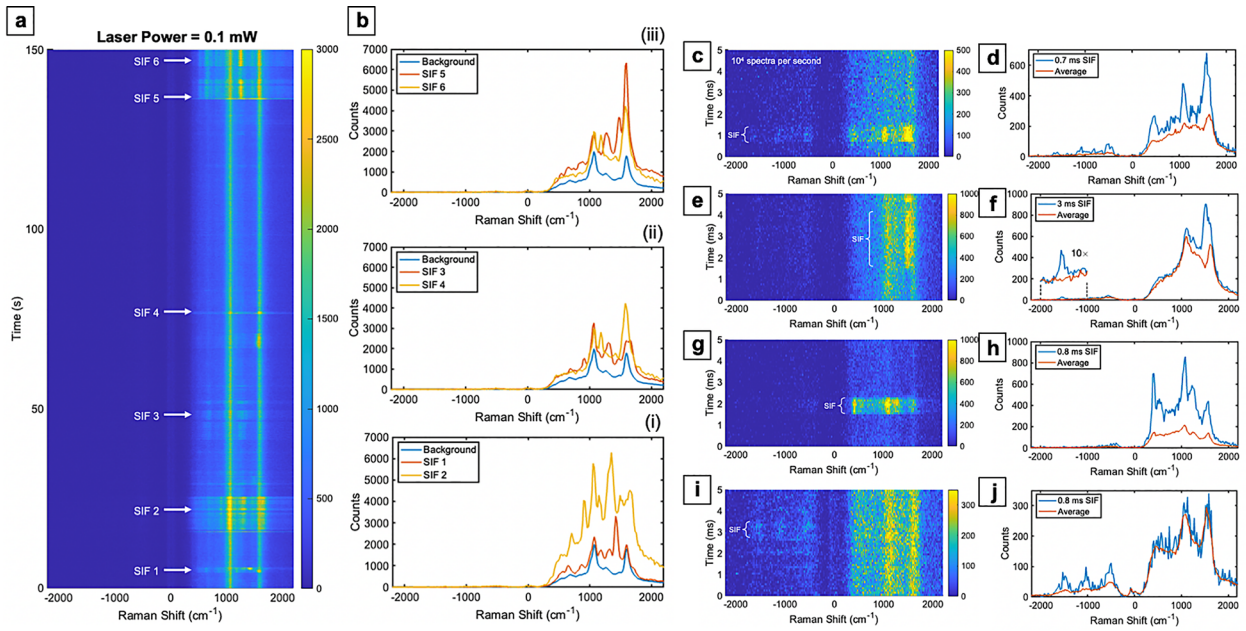

Figure 5. High-speed spectral acquisition of SIFs. (a) An example of an extended slower-speed time-series scan over 150 s to demonstrate sample stability with various SIF events. A 660 nm excitation laser was used with a power of ∼0.1 mW at the sample. (b) Six sample "slow" SIF event spectra compared with the background SERS spectrum. (c−j) Four sample "fast" SIF events with spectral data acquired at 10^4 spectra per second. (c) Waterfall plot showing a single SIF event that occurs in (d) both the Stokes and anti-Stokes spectral regions. (e) Waterfall plot showing a single SIF event that occurs as (f) a single peak in both the Stokes and anti-Stokes regions (at approximately ±1570 cm^{-1}). (g) Waterfall plot showing a single SIF event that mostly occurs in (h) the Stokes region. (i) Waterfall plot showing a single SIF event that mostly occurs in (j) the anti-Stokes region. Figure adapted with permission from ref 26. Copyright 2023 American Chemical Society.

three separate events that occurred less than 10 nm from each other and at different times. Figure 4e shows the SIF intensities plotted in space over the surface of the nanoparticle. These spatial data showed that even a carefully designed SERS substrate, Ag nanoshells in this case, can be very inhomogeneous at the ∼nm level. Indeed, taken together, high-speed acquisition coupled with super-resolution imaging further cements a surprising effect that has been known in SERS research for some time, namely that only very small regions of a SERS substrates are "single-molecule active" yet contribute to a large fraction of the overall SERS signal.[40]

SIFs emitted from the nanoparticle sample were both erratic and brief, providing greater insight into the nature of SERS hotspots and their time dynamics and pointing to the multifaceted, complex interplay of the underlying physical mechanisms behind single-molecule SERS fluctuations. Many more questions must be addressed, such as identifying potential trends in signal fluctuations and their causative factors. For example, Figure 4f,g investigated the role of excitation laser wavelength in SIF behavior. A dry, fully coated Ag nanoshell sample was excited simultaneously by both a 543 nm laser and a 633 nm laser, and the resulting SERS signals were spectrally separated onto two PMT detectors.[20] The resulting two graphs, i.e., the red vs green SERS trajectories, show differences between the SIFs produced by the two excitation wavelengths, as there is a set of SIF events that were excited by only the green laser, a set of SIF events that were excited by only the red laser, and a set of SIF events that were excited by both. These differences suggest that more variables are at play in the SERS mechanism than simply the position of the overall surface plasmon resonance (SPR) of the nanoparticle surface. It is therefore important to investigate the spectral characteristics of SIF excitation.[41] Therefore, while overall high-speed SERS intensity fluctuations provide insight into general hotspot activity, high-speed *spectral* information has the potential to elucidate more of the hotspot behavior, the probe molecule bond activity, and the dynamic nature of light−matter interaction.

Figure 5 shows data from a SERS acquisition system that combines the benefits of high-speed signal acquisition along with spectral information by collecting at a rate of up to 100000 SERS spectra per second.[26] To begin with, Figure 5a first displays a slower spectral SERS scan over the course of 150 s, with six notable SIF events marked. The spectra of these events are displayed in Figure 5b in comparison to the background or average SERS signal of the entire scan. These scans show the appearance of peaks in the spectrum, along with significant overall intensity fluctuations. Interestingly, while it is clear that SIF events do occur over these slower time scales (∼seconds to ∼minutes), high-speed spectroscopy measurements continue to reveal faster and faster spectral fluctuation behavior. These high-speed SIFs were characterized based on a variety of parameters such as duration and, notably, the spectral regions of enhancement. Figure 5c,d displays an SIF characterized as happening in both the Stokes and anti-Stokes regions of the spectrum, hypothetically caused by a molecule entering a hotspot or a hotspot appearing at the location of a molecule. The spectral width of the localized hotspot resonance must be wide enough to enhance the entire SERS spectrum. Figure 5e,f displays a SIF characterized as enhancing a single peak in both the Stokes and anti-Stokes regions, hypothetically caused by an extremely localized hotspot exciting only a single vibrational mode, as in the picocavity regime.[7] Figure 5g,h displays a SIF characterized as happening predominantly in the Stokes region, hypothetically caused by a hotspot with red-shifted resonance. Finally, Figure

https://doi.org/10.1021/acsnano.4c09483
ACS Nano 2024, 18, 25930−25938

5i,j displays a SIF characterized as happening predominantly in the anti-Stokes region, hypothetically caused by a hotspot with blue-shifted resonance. These scans indicate the importance of high-speed spectral data in understanding hotspot behavior and the complex interplay of the many effects that cause SM-SIFs. The anomalously large anti-Stokes peaks are of particular interest for further investigation. Overall, individual SIFs were observed to occur over tens to hundreds of microseconds, enhancing different portions of the SERS spectrum. However, the SIF events overall did not favor a specific region of the spectrum, occurring with roughly equal probability across a wide range, covering both the anti-Stokes and Stokes sides of the spectrum. Along with the high-speed imaging discussed above, these experiments reveal that SM-SERS and SIF events have complex spatial, spectral, and temporal behaviors.

OUTLOOK AND CONCLUSION

SM-SERS has become a rich area for scientific research and discovery, providing exciting possibilities to better understand the fundamental activities and characteristics of plasmonic hotspots and light−matter interactions. It is also full of exciting applications, for example, as a technology to detect very low concentrations of analytes in biological and environmental samples, potentially allowing for earlier and more accurate diagnostics. These capabilities are of particular interest in the field of healthcare, where improving diagnostics has the potential to save lives. SM-SERS has been successfully used for high-sensitivity detection of immune toxicity biomarkers during immune checkpoint inhibitor treatment in cancer patients at concentrations as low as the attomolar level, resulting in highly specific, high-throughput parallel assays and earlier detection of adverse therapy responses.[42] The rapid-response of SERS provides opportunities for point-of-care diagnostic development and ongoing monitoring of disease states. SM-SERS has also been proposed as a method for DNA sequencing[36,43] and single-molecule protein sensing.[44] In addition, the label-free nature of Raman spectroscopy offers a lower-cost solution in comparison to antibody-tagged diagnostics and stain-required histology analysis. SERS diagnostics can identify the presence of multiple analytes quickly with high specificity, without staining, and at low analyte concentration. With the rise of artificial intelligence and machine learning capabilities in data analysis, interpreting complex Raman spectra[45] may allow diagnosing difficult-to-detect diseases such as early stage bladder cancer, far earlier than the current medical standard, using a single drop of sample.[46] Artificial intelligence also shows promise to aid in data collection, postprocessing, and interpretation[47,48] of the complex signals and aid our understanding of the fundamental causative factors of SM-SERS fluctuations.

While SM-SERS is indeed an exciting phenomenon full of potential, significant challenges remain. It is still difficult to mass-produce reliable SERS substrates with high sensitivity. The interpretation of the exact source of all signal fluctuations remains obscured in important ways. Given the erratic nature of SM-SERS, the fundamental metric of SERS, i.e., the so-called "enhancement factor", is difficult to quantify. Experimental challenges also need to be overcome in building higher-speed detectors, spectrometers, and imaging arrays. SM-SERS therefore represents well the challenges and opportunities of fields as disparate as nanophotonics, nanobiosensing, nanotechnology, materials science, and fundamental light−matter interaction. Even after decades of research, it is still a field that is ripe for discovery.

AUTHOR INFORMATION

Corresponding Authors

Alexandre G. Brolo − *Department of Chemistry, University of Victoria, Victoria, British Columbia V8P 5C2, Canada;* orcid.org/0000-0002-3162-0881; Email: agbrolo@uvic.ca

Nathan C. Lindquist − *Department of Physics and Engineering, Bethel University, St Paul, Minnesota 55112, United States;* orcid.org/0000-0002-1226-5212; Email: n-lindquist@bethel.edu

Author

Makayla Maxine Schmidt − *Department of Physics and Engineering, Bethel University, St Paul, Minnesota 55112, United States;* orcid.org/0000-0003-2814-579X

Complete contact information is available at: https://pubs.acs.org/10.1021/acsnano.4c09483

Author Contributions

The manuscript was written through contributions of all authors. All authors have given approval to the final version of the manuscript.

Funding

N.C.L. acknowledges support from the National Science Foundation (NSF) award 2003750. A.G.B. acknowledges Natural Sciences and Engineering Research Council of Canada (NSERC) Discover Grant Awards.

Notes

The authors declare no competing financial interest.

ABBREVIATIONS

SERS, surface-enhanced Raman spectroscopy; SM-SERS, single-molecule surface-enhanced Raman spectroscopy; SIFs, SERS intensity fluctuations; BZT, benzenethiol; FoN, film-over nanosphere; R6G, rhodamine 6G; DTNB, 5,5′-dithiobis-(2-nitrobenzoic acid); TERS, tip-enhanced Raman spectroscopy; STORM, stochastic optical reconstruction microscopy; PMT, photomultiplier tube; SPR, surface plasmon resonance

REFERENCES

(1) Fleischmann, M.; Hendra, P. J.; McQuillan, A. J. Raman Spectra of Pyridine Adsorbed at a Silver Electrode. *Chem. Phys. Lett.* **1974**, *26*, 163−166.

(2) Nam, J.-M.; Oh, J.-W.; Lee, H.; Suh, Y. D. Plasmonic Nanogap-Enhanced Raman Scattering with Nanoparticles. *Acc. Chem. Res.* **2016**, *49*, 2746−2755.

(3) Yamamoto, Y. S.; Itoh, T. Why and How Do the Shapes of Surface-Enhanced Raman Scattering Spectra Change? Recent Progress from Mechanistic Studies. *J. Raman Spectrosc.* **2016**, *47*, 78−88.

(4) Ding, S.-Y.; Yi, J.; Li, J.-F.; Ren, B.; Wu, D.-Y.; Panneerselvam, R.; Tian, Z.-Q. Nanostructure-Based Plasmon-Enhanced Raman Spectroscopy for Surface Analysis of Materials. *Nat. Rev. Mater.* **2016**, *1*, 1−16.

(5) Mosier-Boss, P. A. Review of SERS Substrates for Chemical Sensing. *Nanomaterials* **2017**, *7*, 142.

(6) Azziz, A.; Safar, W.; Xiang, Y.; Edely, M.; de la Chapelle, M. L. Sensing Performances of Commercial SERS Substrates. *J. Mol. Struct.* **2022**, *1248*, 131519.

(7) Benz, F.; Schmidt, M. K.; Dreismann, A.; Chikkaraddy, R.; Zhang, Y.; Demetriadou, A.; Carnegie, C.; Ohadi, H.; De Nijs, B.;

Esteban, R.; Aizpurua, J.; Baumberg, J. J. Single-Molecule Optomechanics in "Picocavities". *Science* **2016**, *354*, 726−729.
(8) Kneipp, K.; Kneipp, H.; Itzkan, I.; Dasari, R. R.; Feld, M. S. Ultrasensitive Chemical Analysis by Raman Spectroscopy. *Chem. Rev.* **1999**, *99*, 2957.
(9) Le Ru, E.; Etchegoin, P.; Meyer, M. Enhancement Factor Distribution Around a Single Surface-Enhanced Raman Scattering Hot Spot and Its Relation to Single Molecule Detection. *J. Chem. Phys.* **2006**, *125*, 204701.
(10) Baumberg, J. J. Picocavities: A Primer. *Nano Lett.* **2022**, *22*, 5859−5865.
(11) dos Santos, D. P.; Temperini, M. L.; Brolo, A. G. Intensity Fluctuations in Single-Molecule Surface-Enhanced Raman Scattering. *Acc. Chem. Res.* **2019**, *52*, 456−464.
(12) Kneipp, K.; Wang, Y.; Kneipp, H.; Perelman, L. T.; Itzkan, I.; Dasari, R. R.; Feld, M. S. Single Molecule Detection Using Surface-Enhanced Raman Scattering (SERS). *Phys. Rev. Lett.* **1997**, *78*, 1667.
(13) Krug, J. T.; Wang, G. D.; Emory, S. R.; Nie, S. Efficient Raman Enhancement and Intermittent Light Emission Observed in Single Gold Nanocrystals. *J. Am. Chem. Soc.* **1999**, *121*, 9208−9214.
(14) Weiss, A.; Haran, G. Time-Dependent Single-Molecule Raman Scattering as a Probe of Surface Dynamics. *J. Phys. Chem. B* **2001**, *105*, 12348−12354.
(15) Maruyama, Y.; Ishikawa, M.; Futamata, M. Thermal Activation of Blinking in SERS Signal. *J. Phys. Chem. B* **2004**, *108*, 673−678.
(16) Kneipp, K.; Emory, S. R.; Nie, S. Single-Molecule Raman Spectroscopy-Fact or Fiction? *Chimia* **1999**, *53*, 35.
(17) Le Ru, E. C.; Meyer, M.; Etchegoin, P. G. Proof of Single-Molecule Sensitivity in Surface Enhanced Raman Scattering (SERS) by Means of a Two-Analyte Technique. *J. Phys. Chem. B* **2006**, *110*, 1944−1948.
(18) Zrimsek, A. B.; Wong, N. L.; Van Duyne, R. P. Single Molecule Surface-Enhanced Raman Spectroscopy: A Critical Analysis of the Bianalyte versus Isotopologue Proof. *J. Phys. Chem. C* **2016**, *120*, 5133−5142.
(19) Marshall, A. R.; Stokes, J.; Viscomi, F. N.; Proctor, J. E.; Gierschner, J.; Bouillard, J.-S. G.; Adawi, A. M. Determining Molecular Orientation via Single Molecule SERS in a Plasmonic Nano-Gap. *Nanoscale* **2017**, *9*, 17415−17421.
(20) Lindquist, N. C.; de Albuquerque, C. D. L.; Sobral-Filho, R. G.; Paci, I.; Brolo, A. G. High-Speed Imaging of Surface-Enhanced Raman Scattering Fluctuations from Individual Nanoparticles. *Nat. Nanotechnol.* **2019**, *14*, 981−987.
(21) Dos Santos, D. P.; Andrade, G. F.; Temperini, M. L.; Brolo, A. G. Electrochemical Control of the Time-Dependent Intensity Fluctuations in Surface-Enhanced Raman Scattering (SERS). *J. Phys. Chem. C* **2009**, *113*, 17737−17744.
(22) Lindquist, N. C.; Bido, A. T.; Brolo, A. G. Single-Molecule SERS Hotspot Dynamics in Both Dry and Aqueous Environments. *J. Phys. Chem. C* **2022**, *126*, 7117−7126.
(23) Kamp, M.; de Nijs, B.; Kongsuwan, N.; Saba, M.; Chikkaraddy, R.; Readman, C. A.; Deacon, W. M.; Griffiths, J.; Barrow, S. J.; Ojambati, O. S.; et al. Cascaded Nanooptics to Probe Microsecond Atomic-Scale Phenomena. *Proc. Natl. Acad. Sci. U. S. A.* **2020**, *117*, 14819−14826.
(24) Moerner, W.; Shechtman, Y.; Wang, Q. Single-Molecule Spectroscopy and Imaging Over the Decades. *Faraday Discuss.* **2015**, *184*, 9−36.
(25) Lindquist, N. C.; Brolo, A. G. Ultra-High-Speed Dynamics in Surface-Enhanced Raman Scattering. *J. Phys. Chem. C* **2021**, *125*, 7523−7532.
(26) Schmidt, M. M.; Farley, E. A.; Engevik, M. A.; Adelsman, T. N.; Tuckmantel Bido, A.; Lemke, N. D.; Brolo, A. G.; Lindquist, N. C. High-Speed Spectral Characterization of Single-Molecule SERS Fluctuations. *ACS Nano* **2023**, *17*, 6675−6686.
(27) Etchegoin, P. G.; Le Ru, E. A Perspective on Single Molecule SERS: Current Status and Future Challenges. *Phys. Chem. Chem. Phys.* **2008**, *10*, 6079−6089.
(28) Margueritat, J.; Bouhelier, A.; Markey, L.; Colas des Francs, G.; Dereux, A.; Lau-Truong, S.; Grand, J.; Lévi, G.; Félidj, N.; Aubard, J.; Finot, E. Discerning the Origins of the Amplitude Fluctuations in Dynamic Raman Nanospectroscopy. *J. Phys. Chem. C* **2012**, *116*, 26919−26923.
(29) Olson, A. P.; Spies, K. B.; Browning, A. C.; Soneral, P. A.; Lindquist, N. C. Chemically Imaging Bacteria with Super-Resolution SERS on Ultra-Thin Silver Substrates. *Sci. Rep.* **2017**, *7*, 9135.
(30) Emory, S. R.; Jensen, R. A.; Wenda, T.; Han, M.; Nie, S. Re-Examining the Origins of Spectral Blinking in Single-Molecule and Single-Nanoparticle SERS. *Faraday Discuss.* **2006**, *132*, 249−259.
(31) Wrzosek, B.; Kitahama, Y.; Ozaki, Y. SERS Blinking on Anisotropic Nanoparticles. *J. Phys. Chem. C* **2020**, *124*, 20328−20339.
(32) Willets, K. A. Super-Resolution Imaging of SERS Hot Spots. *Chem. Soc. Rev.* **2014**, *43*, 3854−3864.
(33) Richard-Lacroix, M.; Deckert, V. Direct Molecular-Level Near-Field Plasmon and Temperature Assessment in a Single Plasmonic Hotspot. *Light: Sci. Appl.* **2020**, *9*, 1−13.
(34) Zhuang, X. Nano-Imaging with STORM. *Nat. Photonics* **2009**, *3*, 365−367.
(35) Olson, A. P.; Ertsgaard, C. T.; Elliott, S. N.; Lindquist, N. C. Super Resolution Chemical Imaging with Plasmonic Substrates. *ACS Photonics.* **2016**, *3*, 329−336.
(36) Chen, C.; Li, Y.; Kerman, S.; Neutens, P.; Willems, K.; Cornelissen, S.; Lagae, L.; Stakenborg, T.; Van Dorpe, P. High Spatial Resolution Nanoslit SERS for Single-Molecule Nucleobase Sensing. *Nat. Commun.* **2018**, *9*, 1733.
(37) Zhang, W.; Rhodes, J. S.; Moon, K. R.; Knudsen, B. S.; Nokolova, L.; Zhou, A. Imaging of PD-L1 in single cancer cells by SERS-based hyperspectral analysis. *Biomedical Optics Express* **2020**, *11*, 6197−6210.
(38) Chen, X.; Gao, Y.; Zhan, J.; Xia, Q.; Chen, Z.; Zhu, J.-J. Spatiotemporal-Resolved Hyperspectral Raman Imaging of Plasmon-Assisted Reactions at Single Hotspots. *Anal. Chem.* **2022**, *94*, 8174−8180.
(39) De Albuquerque, C. D. L.; Schultz, Z. D. Super-Resolution Surface-Enhanced Raman Scattering Imaging of Single Particles in Cells. *Anal. Chem.* **2020**, *92*, 9389−9398.
(40) Fang, Y.; Seong, N.-H.; Dlott, D. D. Measurement of the Distribution of Site Enhancements in Surface-Enhanced Raman Scattering. *Science* **2008**, *321*, 388−392.
(41) Griffiths, J.; De Nijs, B.; Chikkaraddy, R.; Baumberg, J. J. Locating Single-Atom Optical Picocavities Using Wavelength-Multiplexed Raman Scattering. *ACS Photonics* **2021**, *8*, 2868−2875.
(42) Li, J.; Wuethrich, A.; Sina, A. A.; Cheng, H.-H.; Wang, Y.; Behren, A.; Mainwaring, P. N.; Trau, M. A Digital Single-Molecule Nanopillar SERS Platform for Predicting and Monitoring Immune Toxicities in Immunotherapy. *Nat. Commun.* **2021**, *12*, 1087.
(43) Kneipp, K.; Kneipp, H.; Kartha, V. B.; Manoharan, R.; Deinum, G.; Itzkan, I.; Dasari, R. R.; Feld, M. S. Detection and Identification of a Single DNA Base Molecule Using Surface-Enhanced Raman Scattering (SERS). *Phys. Rev. E* **1998**, *57*, R6281.
(44) Almehmadi, L. M.; Curley, S. M.; Tokranova, N. A.; Tenenbaum, S. A.; Lednev, I. K. Surface Enhanced Raman Spectroscopy for Single Molecule Protein Detection. *Sci. Rep.* **2019**, *9*, 12356.
(45) Lussier, F.; Thibault, V.; Charron, B.; Wallace, G. Q.; Masson, J.-F. Deep Learning and Artificial Intelligence Methods for Raman and Surface-Enhanced Raman Scattering. *TrAC Trends Anal. Chem.* **2020**, *124*, 115796.
(46) Lee, S.; Jue, M.; Lee, K.; Paulson, B.; Oh, J.; Cho, M.; Kim, J. K. Early-Stage Diagnosis of Bladder Cancer Using Surface-Enhanced Raman Spectroscopy Combined with Machine Learning Algorithms in a Rat Model. *Biosens. Bioelectron.* **2024**, *246*, 115915.
(47) Rojalin, T.; Antonio, D.; Kulkarni, A.; Carney, R. P. Machine Learning-Assisted Sampling of Surfance-Enhanced Raman Scattering (SERS) Substrates Improve Data Collection Efficiency. *Appl. Spectrosc.* **2022**, *76*, 485−495.

https://doi.org/10.1021/acsnano.4c09483
ACS Nano 2024, 18, 25930−25938

(48) Kumar, P. P. P.; Kaushal, S.; Lim, D.-K. Recent advances in nano/microfabricated substrate platforms and artificial intelligence for practical surface-enhanced Raman scattering-based bioanalysis. *TrAC Trends in Anal. Chem.* **2023**, *168*, 117341.

https://doi.org/10.1021/acsnano.4c09483
ACS Nano 2024, 18, 25930−25938